AC loss evaluation of MgB_2 superconducting windings located in a stator core slot with a finite-element method

Kajikawa, Kazuhiro
Research Institute of Superconductor Science and Systems, Kyushu University

Osaka, Ryota
Department of Electrical Engineering, Kyushu University

Nakamura, Taketsune
Department of Electrical Engineering, Kyoto University

Sugano, Michinaka
Department of Electronic Science and Engineering, Kyoto University

他

https://hdl.handle.net/2324/25447

出版情報：Journal of Superconductivity and Novel Magnetism. 24 (1/2), pp.987-991, 2011-01-01. Springer US
バージョン：

Title:

AC Loss Evaluation of MgB_2 Superconducting Windings Located in a Stator Core Slot with a Finite Element Method

(Running head: AC Loss Evaluation of MgB_2 Windings with a Finite Element Method)

Authors:

Kazuhiro Kajikawa, Ryota Osaka, Taketsune Nakamura, Michinaka Sugano, Tsuyoshi Wakuda

Affiliations:

K. Kajikawa

Research Institute of Superconductor Science and Systems, Kyushu University, Fukuoka 819-0395, Japan

e-mail: kajikawa@sc.kyushu-u.ac.jp

R. Osaka

Department of Electrical Engineering, Kyushu University, Fukuoka 819-0395, Japan

T. Nakamura

Department of Electrical Engineering, Kyoto University, Kyoto 615-8510, Japan

M. Sugano

Department of Electronic Science and Engineering, Kyoto University, Kyoto 615-8510, Japan

T. Wakuda

Hitachi Research Laboratory, Hitachi, Ltd., Hitachi 319-1292, Japan

Abstract:

AC losses in stator windings of fully superconducting motors with an MgB_2 wire are numerically evaluated by means of a finite element method using edge elements for self magnetic field. The physical properties of the MgB_2 wire for numerical calculations are obtained from the corresponding experiments with an existing wire. It is assumed that the voltage-current characteristics of the MgB_2 wire are given by Bean's critical state model, in which the critical current density is independent of the local magnetic field. The influences of core slot size and turn number of windings on the AC losses are discussed quantitatively toward the optimum design of the stator winding with the MgB_2 wire.

Keywords:

AC loss, Finite element analysis, Magnesium diboride, Stator winding, Superconducting motor

Corresponding author:

Prof. Kazuhiro Kajikawa

Research Institute of Superconductor Science and Systems, Kyushu University, 744 Motooka, Nishi-ku, Fukuoka 819-0395, Japan

Phone: +81-92-802-3836, Fax: +81-92-802-3829, E-mail: kajikawa@sc.kyushu-u.ac.jp

1. INTRODUCTION

Hydrogen is one of the promising energy mediums in the near future because its oxidization yields only water as a by-product. In order to ensure that hydrogen is handled safely and stably, the total system for its production, transportation, storage, and transfer must be established as an important infrastructure for a sustainable society. However, because of its small mass density, it requires effective treatment, especially during transportation and in storage. Hence, liquid hydrogen is preferred to compressed hydrogen because the density of the former is much larger than that of the latter.

In the last decade, an MgB_2 superconductor with the critical temperature of 39 K [1] has been known as one of the promising materials used in the liquid hydrogen, which has the boiling temperature of about 20 K at atmospheric pressure. Although many MgB_2 superconducting wires with metal sheaths have been fabricated up to now, the critical current densities of the present MgB_2 wires at 20 K decrease drastically in an external magnetic field of a few teslas [2]. This implies that the present MgB_2 wires would be suitable for applications in low magnetic fields. As one of the low-field applications of MgB_2 wires, a fully superconducting motor has been proposed to drive an electric pump used for the circulation or transfer of liquid hydrogen [3]. Since the MgB_2 superconducting windings for the rotor and stator in the motor are placed inside iron cores, the windings are scarcely exposed to the external magnetic field, and therefore, self-fields generated by the currents flowing in the windings themselves become dominant. Three-phase alternating currents are supplied to the stator winding in the proposed motor to generate a rotating magnetic field, so that a detailed understanding of the AC loss properties of MgB_2 windings is one of the key factors to realize a cryogenic superconducting pump.

In this study, the AC losses in MgB_2 stator windings for fully superconducting motor are numerically evaluated by means of a finite element method [4]. The influences of core slot size and turn number of windings on the AC losses are quantitatively discussed as compared with those for a conventional copper winding.

2. NUMERICAL CALCULATIONS OF AC LOSSES

Let us consider one of slots in an iron core for stator with two layer windings and additionally a small gap to a rotor core as shown in Fig. 1(a). When the transport currents with two different phases, e.g. phase b and c, are applied to the stator windings, the typical lines of magnetic force around the stator core slot can be depicted as shown in Fig. 1(a). If the permeability of iron cores can be regarded as infinity, the lines of force always become normal to the surfaces of the cores. Therefore, a numerical model in Fig. 1(b) can be considered for a half part of the stator core slot for the sake of symmetry. Each stator winding is composed of N turns of a superconducting wire with the corresponding transport current, and an example of $N = 2$ is drawn in Fig. 1(b). The symbols, d and w, denote the depth and half width of the stator core slot, respectively, and the gap length between the stator and rotor cores is represented by the symbol g. The three-phase currents are also symbolized by i_a, i_b, and i_c for phase a, b, and c, respectively. The tangential component H_t of magnetic field on the closed path C surrounding the entire analysis area is equal to zero because of the characteristics of the lines of magnetic force as shown in Fig. 1(a) except for that in the gap part, H_g. The paths C_1 and C_2 on the surface of every superconducting wire in the inner and outer windings are used for applying i_b and i_c, respectively, as mentioned later.

In order to obtain the distribution of electromagnetic fields in the numerical model as shown in Fig. 1(b), the finite element analysis formulated with a self magnetic field due to induced currents [4] is carried out as follows. In this method, the governing equation is expressed by

$$\nabla \times \left(\rho \nabla \times \boldsymbol{H}_s\right) = -\mu_0 \frac{\partial}{\partial t}\left(\boldsymbol{H}_s + \boldsymbol{H}_e\right), \tag{1}$$

where ρ is the electrical resistivity of each material, and the local magnetic field is given by the sum of the self-field $\boldsymbol{H}_s$ and a uniform external applied field $\boldsymbol{H}_e$. In the numerical model as shown in Fig. 1(b), the external field $\boldsymbol{H}_e$ can be considered equal to zero because the magnetic flux generated by the remaining stator windings in the other slots passes through only the teeth parts of the cores. When both the Galerkin method for edge elements [5] and the backward difference method for time are applied to discretize Eq. (1), a set of simultaneous equations can be derived. Since the sum of three-phase currents is equal to zero as

$$i_a + i_b + i_c = 0 , \tag{2}$$

the line integral of the self-field $\boldsymbol{H}_s$ on the closed path C surrounding the entire analysis area becomes

$$\oint_{\mathrm{C}} \boldsymbol{H}_s \cdot \mathrm{d}\boldsymbol{s} = -H_g g = \frac{Ni_b + Ni_c}{2} = -\frac{Ni_a}{2} . \tag{3}$$

The following restraint conditions on the paths C$_1$ and C$_2$ are also taken into account,

$$\oint_{\mathrm{C}_1} \boldsymbol{H}_s \cdot \mathrm{d}\boldsymbol{s} = \frac{i_b}{2} , \quad \oint_{\mathrm{C}_2} \boldsymbol{H}_s \cdot \mathrm{d}\boldsymbol{s} = \frac{i_c}{2} . \tag{4}$$

If the voltage-current characteristics are represented by Bean’s critical state model [6], in which the critical current density is independent of the local magnetic field, the resistivity ρ_s for superconductor is expressed by [4]

$$
\rho_s = \begin{cases} 0, & |\boldsymbol{J}| \le J_c, \\ \rho_f \left(1 - \dfrac{J_c}{|\boldsymbol{J}|} \right), & |\boldsymbol{J}| > J_c, \end{cases} \tag{5}
$$

where ρ_f is the flux-flow resistivity, $\boldsymbol{J}$ the local current density given by $\boldsymbol{J} = \nabla \times \boldsymbol{H}_s$, and J_c the critical current density of the superconductor. Since the resistivity ρ_s for superconductor is as a function of the self-field $\boldsymbol{H}_s$, the simultaneous equations derived from Eq. (1) become nonlinear and therefore iterative calculations with the Newton-Raphson method are carried out at each time step. By using the obtained time evolution of the self-field distribution, the AC loss W per unit volume per cycle is numerically evaluated by

$$
W = \frac{1}{S} \oint \mathrm{d}t \int_{\mathrm{S}} \rho |\nabla \times \boldsymbol{H}_s|^2 \, \mathrm{d}S \,, \tag{6}
$$

where S is the cross-sectional area of the material under consideration with the region S.

3. PARAMETERS FOR NUMERICAL CALCULATIONS

In order to investigate the effect of the replacement of copper stator windings with superconducting windings on the loss reduction, a typical conventional induction motor as shown in Table I is focused on [7]. The rated output power of this motor is 1.5 kW, and the numbers of phase and pole are three and four, respectively. The rated voltage and frequency f are 200 V and 60 Hz, respectively. The number of the stator core slot is 36, and its typical length ℓ, width and depth are 88 mm, 4.4 mm and 12 mm, respectively. The gap length g between the stator and rotor iron cores is 0.5 mm. The magnetomotive force and resistance of primary copper winding are given by 165.5 A and 1.21 Ω, respectively.

Table II lists the basic parameters of numerical calculations with the finite element method. The superconducting wire is in existence and has a single filament of MgB_2 superconductor surrounded by niobium and copper sheaths [8]. The diameters of wire and filament are 0.8 mm and 0.555 mm, respectively, and the outer diameter of niobium is 0.685 mm. The operating temperature is assumed to be 20 K, so that the critical current I_c of this wire has been estimated as 336 A in the self-field. The resistivity of niobium is 0.51 μΩ·cm at 20 K, and the corresponding resistivity for copper is 0.01 μΩ·cm. It is also assumed that the flux-flow resistivity ρ_f is equal to 10 μΩ·cm [4]. If the basic profiles for the superconducting motor such as the core size and magnetomotive force are identical to those for the conventional induction motor, it is enough to prepare one turn or two turns of the superconducting wire as the stator windings because of its high current capacity. In this case, the rated primary current I_e becomes 165.5 A or 82.7 A for $N = 1$ or 2, so that the load factor i_m of the current amplitude I_m divided by the critical current I_c equals to 0.70 or 0.35, respectively. On the other hand, the width and depth of the stator core slot are varied so as to decrease the internal empty space due to the high current density of the superconducting windings.

4. NUMERICAL RESULTS OF AC LOSSES

Fig. 2(a) shows the comparison among the numerical results of AC losses per unit volume per cycle for respective materials constituting the superconducting wire. The width $2w$ and depth d of the stator core slot are fixed at 4.4 mm and 12 mm, respectively. The AC losses in the superconductor filament are always the largest, but the losses in the copper sheath are quite large and comparable to them. This is due to the eddy current losses in the copper sheath material [8]. On the other hand, the losses in the niobium sheath are small and negligible. The numerical results of the AC losses per unit volume of the wire per cycle, W_w, are converted into the equivalent primary resistances R per phase as shown in Fig. 2(b) by using the equation,

$$R = \frac{24 W_w N S_w 1 f}{I_e^2}\ , \tag{7}$$

where S_w is the cross-sectional area of the superconducting wire. The primary resistance for the conventional copper winding at 20 K is also presented in Fig. 2(b) under the assumption that the residual resistance ratio (RRR), which is defined here by the ratio of the resistance at an operating temperature of the conventional motor to the resistance at 20 K, is a hundred for the copper. The skin effect for cyclic field due to very low resistivity of the normal metal at cryogenic temperature is not taken into account. It can be seen that the equivalent resistances in the superconducting windings are more than two orders of magnitude smaller than the primary resistance of the copper winding cooled down to 20 K.

Fig. 3 shows the dependence of the numerical results of AC losses on the size of stator core slot carried out for the purpose validating the possibility of decrease in the void inside it. The AC losses as a function of the slot width $2w$ are plotted in Fig. 3(a), where the slot depth is fixed at 12 mm. It is found that the AC losses increase somewhat with decreasing the width of the stator core slot. On the other hand, the AC losses for the depth d of the stator core slot are given in Fig. 3(b), where the slot width is constant at 4.4 mm. In this case, the AC losses scarcely depend on the slot depth but slightly increase with decreasing it.

Fig. 4 shows the numerical results of AC losses as a function of the turn number of stator winding, N. Since the cross-sectional area of both the superconducting wire and filament are maintained at a constant for single or double of the existing wire as already given in Table II, the load factor i_m of the current amplitude I_m to the critical current I_c is equal to 0.70 or 0.35, respectively. It can be seen that the AC losses decrease with increasing the turn number of stator winding. This means that the reduction of the diameter of superconducting wire is effective for the suppression of the AC loss and the increase in the efficiency of the superconducting motor.

5. CONCLUSIONS

The AC losses in the stator windings of the superconducting motor at the liquid hydrogen temperature were numerically evaluated by means of the finite element method formulated with the self magnetic field due to the current induced in the analysis region. It was expected that the use of the present MgB_2 superconducting wire contributed to suppressing the primary power consumption by about two orders of magnitude smaller than that for the copper winding cooled down to the identical temperature. Such a prospective property would be validated experimentally for a fabricated MgB_2 stator winding immersed in the liquid helium and surely with the liquid hydrogen in the near future.

Acknowledgements

This work was supported by the Industrial Technology Research Grant Program in 2008 (08B38006a) from the New Energy and Industrial Technology Development Organization (NEDO) of Japan.

References

1. J. Nagamatsu, N. Nakagawa, T. Muranaka, Y. Zenitani, and J. Akimitsu, Nature 410, 63 (2001).
2. M. Tomsic, M. Rindfleisch, J. Yue, K. McFadden, D. Doll, J. Phillips, M. D. Sumption, M. Bhatia, S. Bohnenstiehl, and E. W. Collings, Physica C 456, 203 (2007).
3. K. Kajikawa and T. Nakamura, IEEE Trans. Appl. Supercond. 19 1669 (2009).
4. K. Kajikawa, T. Hayashi, R. Yoshida, M. Iwakuma, and K. Funaki, IEEE Trans. Appl. Supercond. 13, 3630 (2003).
5. J. Jin, The Finite Element Method in Electromagnetics, 2nd Ed. (John Wiley & Sons, New York, 2002).
6. C. P. Bean, Phys. Rev. Lett. 8, 250 (1962).
7. T. Nakamura, Y. Ogama, H. Miyake, K. Nagao, and T. Nishimura, Supercond. Sci. Technol. 20, 911 (2007).
8. K. Kajikawa, T. Kawano, R. Osaka, T. Nakamura, M. Sugano, M. Takahashi, and T. Wakuda, Supercond. Sci. Technol. 23, 045026 (2010).

Table I Specifications of conventional induction motor [7].

Rated output power	1.5 kW
Number of phase/pole	3/4
Rated voltage	200 V
Frequency, f	60 Hz
Number of stator core slot	36
Length of stator core slot, ℓ	88 mm
Typical width of stator core slot	4.4 mm
Typical depth of stator core slot	12 mm
Gap between stator and rotor cores, g	0.5 mm
Magnetomotive force of primary winding	165.5 A
Primary resistance	1.21 Ω
Synchronous rotating speed	1,800 rpm
Rated rotating speed	1,720 rpm

Table II Basis parameters for numerical calculations.

Structure of superconducting wire	MgB_2/Nb/Cu
Number of filament	1
Diameter of wire	0.8 mm
Diameter of filament	0.555 mm
Outer diameter of Nb	0.685 mm
Operating temperature	20 K
Critical current, I_c	336 A
Resistivity of Nb	0.51 μΩ·cm
Resistivity of Cu	0.01 μΩ·cm
Flux-flow resistivity, ρ_f	10 μΩ·cm
Magnetomotive force of primary winding, NI_e	165.5 A
Turn number of primary winding, N	1 or 2
Load factor, $i_m = I_m/I_c$	0.70 or 0.35
Width of stator core slot, $2w$	1.6, 2.4, or 4.4 mm
Depth of stator core slot, d	4, 6, 8, 10, or 12 mm

Figure captions:

Fig. 1 Schematic diagram of (a) lines of magnetic force around one of slots in stator iron core with two layer windings and (b) numerical modeling for half core slot.

Fig. 2 Comparison among (a) numerical results of AC losses for respective materials constituting superconducting wire and (b) equivalent primary resistances for superconducting windings and copper winding cooled down to 20 K.

Fig. 3 Dependence of numerical results of AC losses on (a) width and (b) depth of stator core slot. The depth of core slot in (a) and the width in (b) are fixed at 12 mm and 4.4 mm, respectively.

Fig. 4 Dependence of numerical results of AC losses on turn number of stator windings. The width and depth of core slot are fixed at 4.4 mm and 12 mm, respectively. The total cross-sectional area of superconductor filaments in the windings is maintained constant in each case.

S-P-073 / ICSM2010, K. Kajikawa et al., Fig. 1

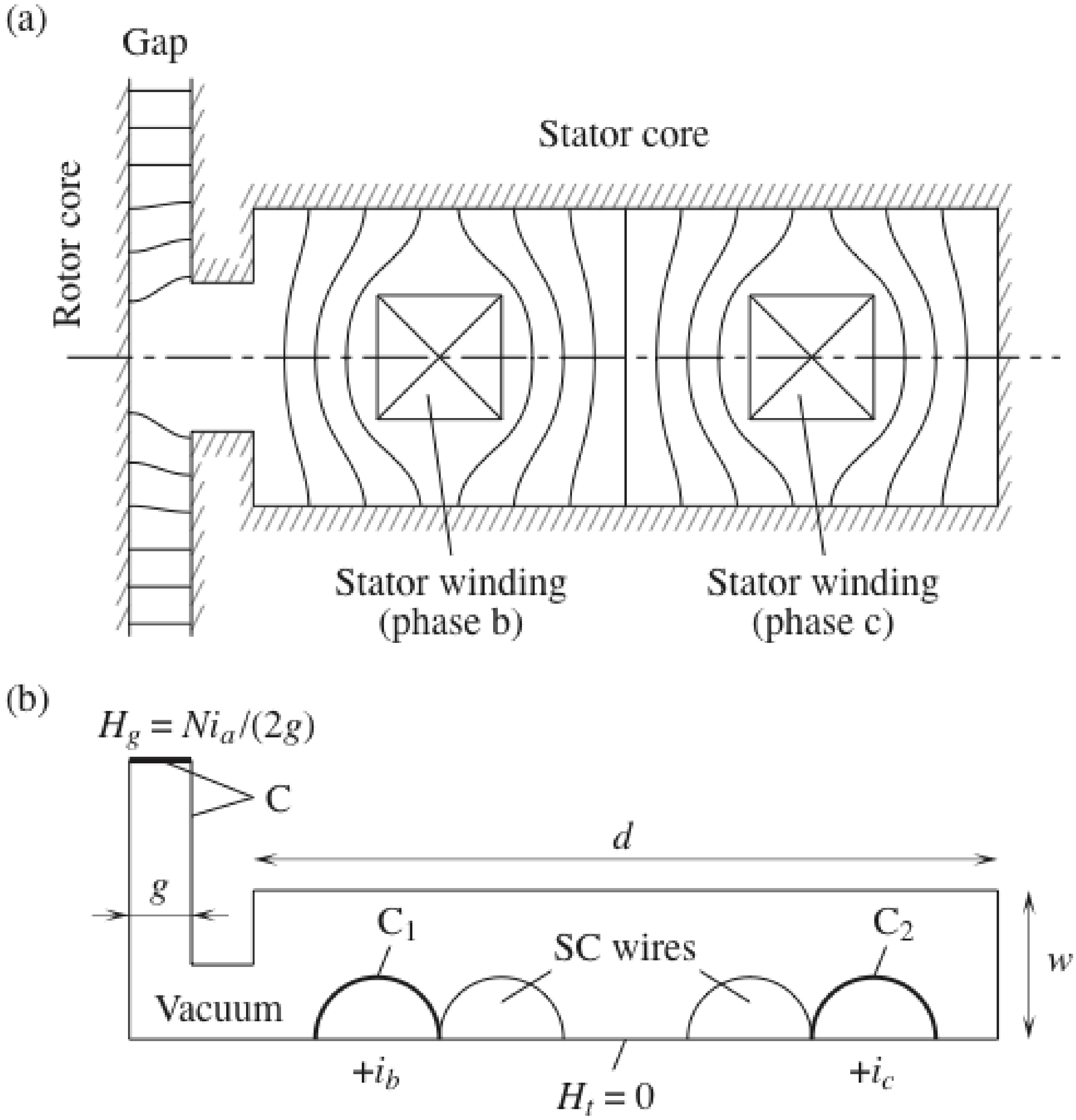

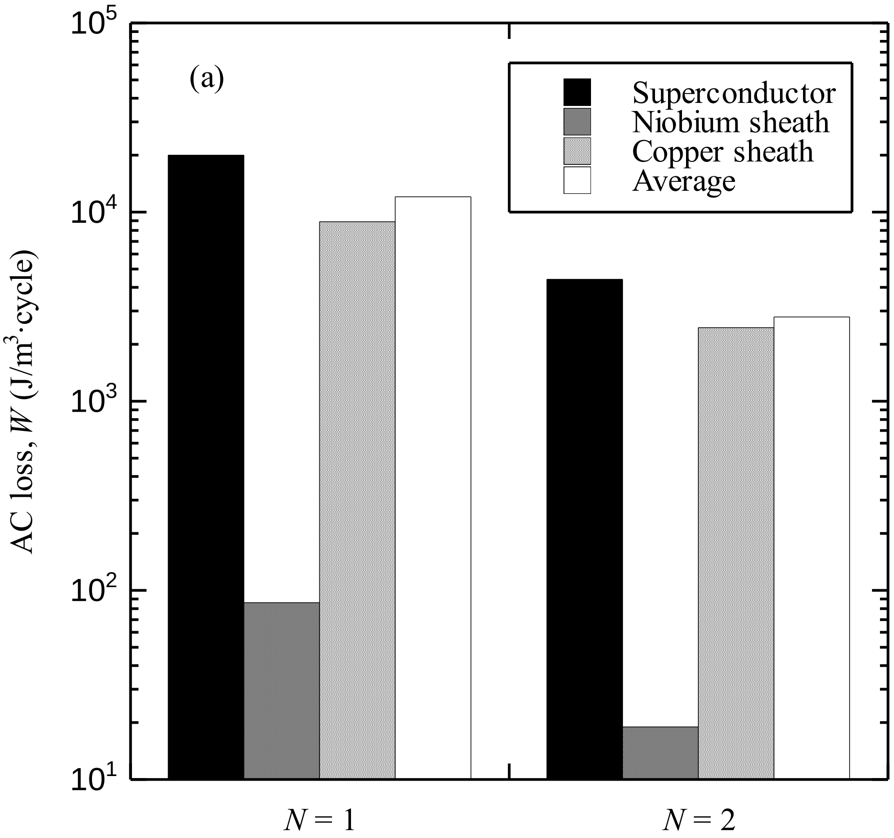
(a)
Superconductor
Niobium sheath
Copper sheath
Average
AC loss, W (J/m^3·cycle)
10^5
10^4
10^3
10^2
10^1
$N = 1$
$N = 2$

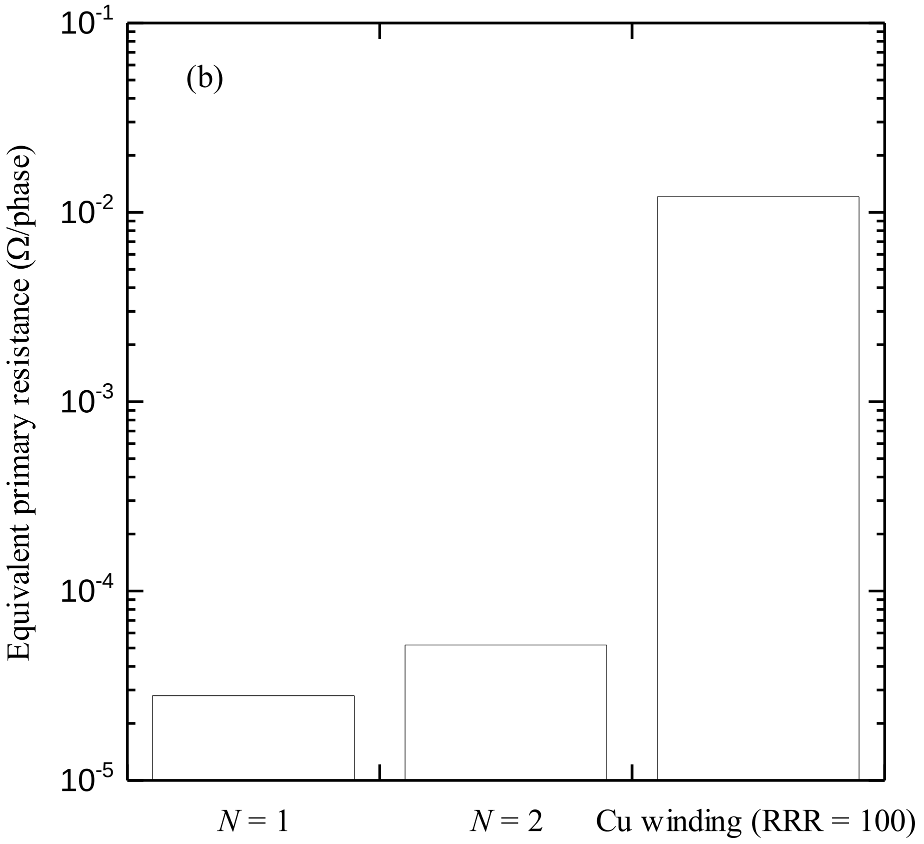
(b)
Equivalent primary resistance (Ω/phase)
10^{-1}
10^{-2}
10^{-3}
10^{-4}
10^{-5}
N = 1
N = 2
Cu winding (RRR = 100)

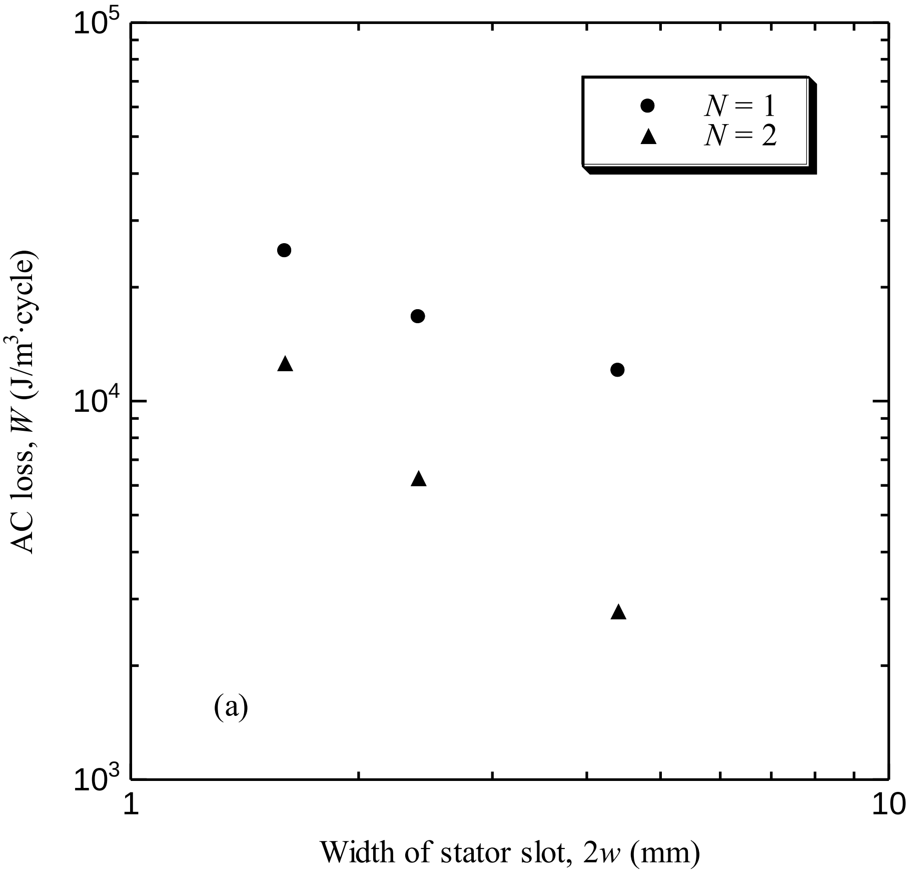
10^5
10^4
10^3
1
10
AC loss, W (J/m^3·cycle)
Width of stator slot, 2w (mm)
● $N = 1$
▲ $N = 2$
(a)

S-P-073 / ICSM2010, K. Kajikawa et al., Fig. 3(b)

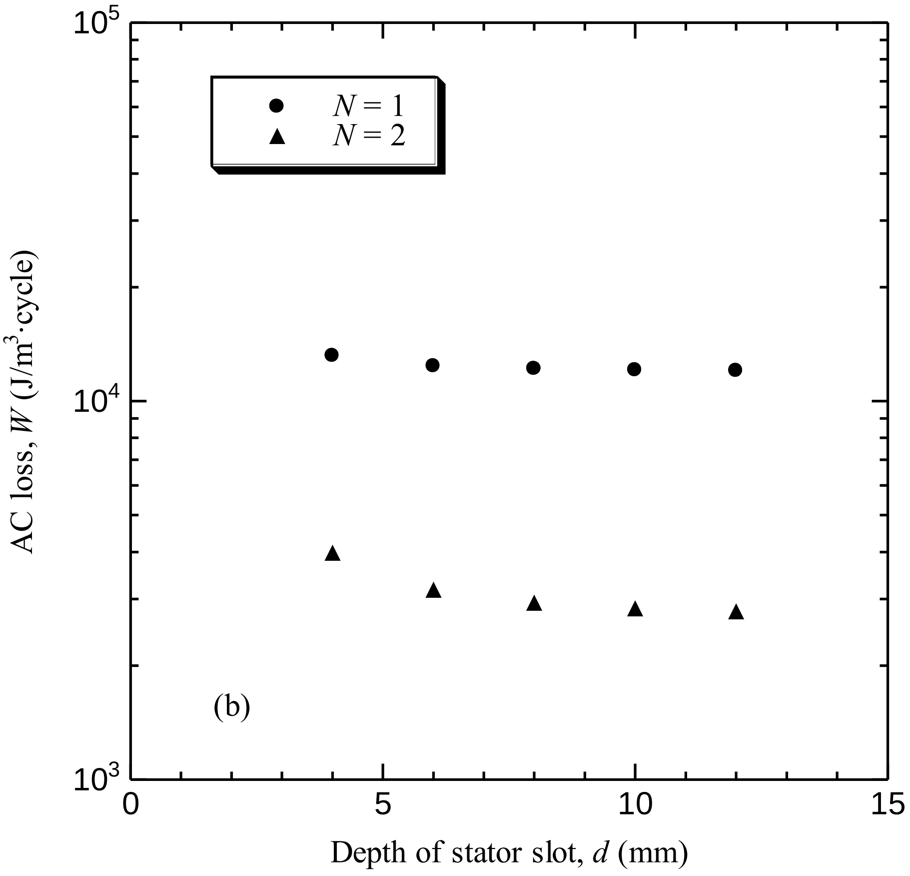

S-P-073 / ICSM2010, K. Kajikawa et al., Fig. 4